International Journal of Minerals, Metallurgy and Materials
Volume 23, Number 9, September 2016, Page 1001
DOI: 10.1007/s12613-016-1317-x

Kinetics of petroleum coke/biomass blends during co-gasification

Jian-liang Zhang, Jian Guo, Guang-wei Wang, Tao Xu, Yi-fan Chai, Chang-le Zheng, and Run-sheng Xu

School of Metallurgical and Ecological Engineering, University of Science and Technology Beijing, Beijing 100083, China

(Received: 8 March 2016; revised: 13 April 2016; accepted: 21 April 2016)

Abstract: The co-gasification behavior and synergistic effect of petroleum coke, biomass, and their blends were studied by thermogravimetric analysis under CO_2 atmosphere at different heating rates. The isoconversional method was used to calculate the activation energy. The results showed that the gasification process occurred in two stages: pyrolysis and char gasification. A synergistic effect was observed in the char gasification stage. This effect was caused by alkali and alkaline earth metals in the biomass ash. Kinetics analysis showed that the activation energy in the pyrolysis stage was less than that in the char gasification stage. In the char gasification stage, the activation energy was 129.1–177.8 kJ/mol for petroleum coke, whereas it was 120.3–150.5 kJ/mol for biomass. We also observed that the activation energy calculated by the Flynn–Wall–Ozawa (FWO) method were larger than those calculated by the Kissinger–Akahira–Sunosen (KAS) method. When the conversion was 1.0, the activation energy was 106.2 kJ/mol when calculated by the KAS method, whereas it was 120.3 kJ/mol when calculated by the FWO method.

Keywords: gasification; petroleum coke; biomass; synergistic effect; kinetics

1. Introduction

Petroleum coke (PC) is a byproduct of delayed coking. With increasing supply of heavy crude oil around the world, PC production has continued to increase [1]. Thus, an effective use for PC needs to be found. Gasification can convert different carbonaceous resources into syngas ($CO + H_2$); such carbonaceous resources include coal, biomass, and PC, and the produced syngas can be applied to DRI production [1]. Therefore, gasification technology is available for effectively using PC [2]. However, PC has high carbon content and is difficult to gasify [3–4]. Higher gasification temperatures and longer gasification times are needed to complete the gasification reaction. Co-gasification can be a good choice to gasify PC [4]. Biomass, as a zero-emission renewable resource [5], exhibits high reactivity and high oxygen content; it can feasibly be used to co-gasify with PC.

Some research on co-gasification has been reported. Zuo *et al.* [6] compared kinetic models for isothermal CO_2 gasification of blended coal char–biomass char. Moreover, catalytic effect of potash on deashing biomass char gasification has been observed [7]. Wang *et al.* [8] studied the CO_2-gasification properties of biomass chars and anthracite char. Edreis *et al.* [9–10] have reported a series of co-gasification experiments involving PC and biomass in different atmospheres, such as CO_2 and H_2O. Nemanova *et al.* [11] researched co-gasification of biomass and PC in a bubbling fluidized bed using a thermogravimetric analyzer. In nonisothermal steam gasification experiments, a synergetic effect between PC and biomass was observed. They further observed that biomass ash had a catalytic effect on the gasification reactivity. Fermoso *et al.* [12–14] investigated the effect of co-gasification of PC, biomass, and coal on the composition of the resulting synthesis gas. They observed a synergetic effect among the components. Xu and Sun [15] studied the effects of gasification modes, PC addition ratio, addition methods, particle size, and gasification temperature on tar production and co-gasification behavior.

In this work, we use a thermogravimetric analyzer to investigate the effect of the blend ratio and heating rate on the gasification behavior. A synergetic interaction between PC and biomass was also studied. Moreover, we investigated CO_2 gasification kinetics of PC, biomass, and their blends

Corresponding author: Guang-wei Wang E-mail: wgw676@163.com

using isoconversional methods. The kinetic parameters obtained via two isoconversional methods are compared.

2. Experimental section

2.1. Materials

PC and biomass were selected as raw materials. Corn cob was used as the biomass. By drying, grinding, and sieving the PC and biomass, their particle sizes were controlled in the range from 74 to 149 μm. The results of proximate and ultimate analyses of the samples are presented in Table 1. The results of ash analyses of the samples are presented in Table 2. PC and biomass were blended in weight proportions of 4:1, 1:1, and 1:4.

Table 1. Proximate and ultimate analysis of PC and biomass wt%

Samples	Proximate analysis			Ultimate analysis				
	A_d	V_d	FC_d	C_d	H_d	O_d	N_d	S_d
PC	3.29	11.14	85.57	85.5	4.2	1.2	1.9	7.2
biomass	2.66	76.62	20.73	45.33	3.7	43.31	0.46	0.14

Note: FC, fixed carbon; A, ash; V, volatile matter; C, H, O, N, S represent carbon, hydrogen, nitrogen and sulfur in the coal respectively. d, dry basis.

Table 2. Ash analysis of PC and biomass wt%

Samples	K_2O	Na_2O	CaO	MgO	SiO_2	Al_2O_3	Fe_2O_3	SO_3	P_2O_5	NiO	V_2O_5
PC	0.30	1.86	31.82	1.62	14.61	11.66	4.58	21.17	1.69	3.58	4.88
biomass	51.2	0.43	3.92	0.99	24.87	1.92	2.2	1.11	0.86	0.09	0.12

2.2. CO_2 gasification experiments

CO_2 gasification of PC, biomass, and their blends was carried out using a thermogravimetric analyzer (HCT-3, Henven Scientific Instrument Factory). The samples, whose masses ranged from 5 to 5.5 mg in each experiment, were heated to 1200°C at a heating rate of 5, 10, or 20°C/min. The flow rate of CO_2 was 100 mL/min. To ensure that the experiments were reproducible, we repeated each run at least three times before a final result was ascertained.

3. Kinetic analysis

The degree of conversion of the gasification process is expressed as

$$\alpha = \frac{m_0 - m_t}{m_0 - m_\infty} \tag{1}$$

where m_0 is the initial mass of the sample; m_t is the mass of the sample at time t; and m_∞ is the final mass of the sample in the reaction.

The rate of the gasification reaction is generally described by the following equation [16]:

$$\frac{\mathrm{d}\alpha}{\mathrm{d}t} = k(T)f(\alpha) \tag{2}$$

where $\mathrm{d}\alpha/\mathrm{d}t$ is the reaction rate; α is the conversion degree; t is the time; T is the absolute temperature; and $f(\alpha)$ describes the reaction kinetics, which depends on the reaction mechanism. Parameter $k(T)$ is the reaction rate constant and is usually described by the Arrhenius equation:

$$k(T) = A\exp\left(-\frac{E}{RT}\right) \tag{3}$$

where A is a frequency factor, E is the activation energy, and R is the universal gas constant.

Thus, the reaction rate can be described as follows:

$$\frac{\mathrm{d}\alpha}{\mathrm{d}t} = A\exp\left(-\frac{E}{RT}\right)f(\alpha) \tag{4}$$

An integration function is shown as below:

$$g(\alpha) = \int_0^\alpha \frac{\mathrm{d}\alpha}{f(\alpha)} = \frac{A}{\beta}\int_{T_0}^{T}\exp\left(-\frac{E}{RT}\right)\mathrm{d}T \tag{5}$$

where $g(\alpha)$ is the integral kinetic function or integral reaction model when its form is mathematically defined and $\beta = \mathrm{d}T/\mathrm{d}t$ is the heating rate of gasification.

In nonisothermal kinetics, a few methods to calculate kinetic data have been developed, such as the Friedman (FR) [17], Kissinger–Akahira–Sunosen (KAS) [18], and the Flynn–Wall–Ozawa (FWO) [19] methods, which differ slightly. In the case of the Friedman method, no mathematical approximations are made. The FWO method is known to be inaccurate [17]. The KAS equation applies a range of approximations for the temperature integral and is known to be more accurate [17].

In this paper, the KAS method was used to calculate the activation energy because of its accuracy. The FWO method was also used to calculate the activation energy of biomass for comparison with the results obtained via the KAS

method. The KAS [18] method is based on the following equation:

$$\ln\left(\frac{\beta}{T^2}\right)=\ln\left[\frac{AR}{E_\alpha g(\alpha)}\right]-\frac{E_\alpha}{RT} \tag{6}$$

For α = const, a plot of $\ln(\beta/T^2)$ vs. $1/T$ using data obtained at several heating rates yields a straight line whose slope enables the calculation of the apparent activation energy.

The E_α for conversion values can be calculated from a plot of $\ln(\beta/T^2)$ vs. $1/T$.

The FWO method [19] is based on the following equation:

$$\ln\beta=\ln\left[\frac{AE_\alpha}{Rg(\alpha)}\right]-5.331-\frac{E_\alpha}{RT} \tag{7}$$

In this case, the E_α for conversion values can be calculated from a plot of $\ln\beta$ vs. $1/T$.

4. Results and discussion

4.1. Gasification characteristics

To investigate the co-gasification of PC and biomass, we performed thermogravimetric tests. CO_2 gasification of different blend ratios was conducted in a thermobalance at different heating rates. The obtained fractional conversion curves and reaction rate curves are illustrated in Figs. 1–3. As evident in these figures, the gasification of biomass can be divided into two stages: pyrolysis and char gasification. The first peak of pyrolysis of all blends appeared at temperatures less than 400°C, and also the shape and position of this peak remained the same for all blends. The second peak of char gasification appeared at temperatures greater than 700°C. However, with increasing ratio of biomass, the position and shape of the peak in the reaction-rate curves changed. In the case of PC, only a char gasification stage was observed.

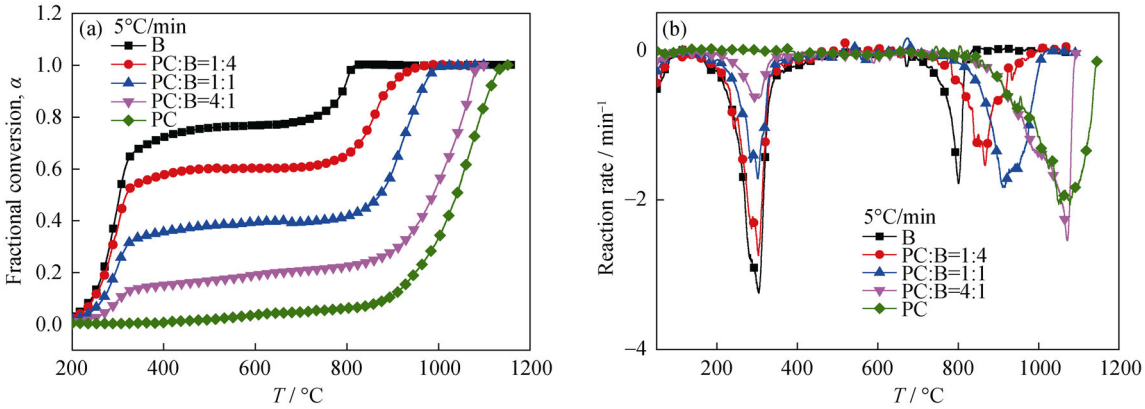

Fig. 1. Effect of blend ratio on the thermal behavior of samples at β = 5°C/min: (a) fractional conversion curves; (b) reaction rate curves.

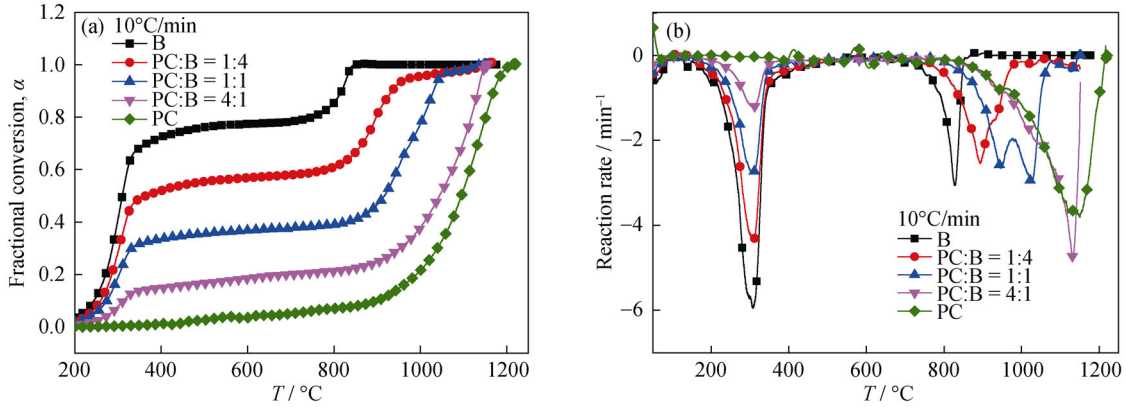

Fig. 2. Effect of blend ratio on the thermal behavior of samples at β = 10°C/min: (a) fractional conversion curves; (b) reaction rate curves.

The co-gasification parameters obtained at different heating rates are summarized in Table 3. The gasification characteristic parameters included DTG_{max}, T_{max} the temperature range, in which the DTG_{max} was the maximum reaction rate, and T_{max} was the temperature corresponding to the maximum reaction rate.

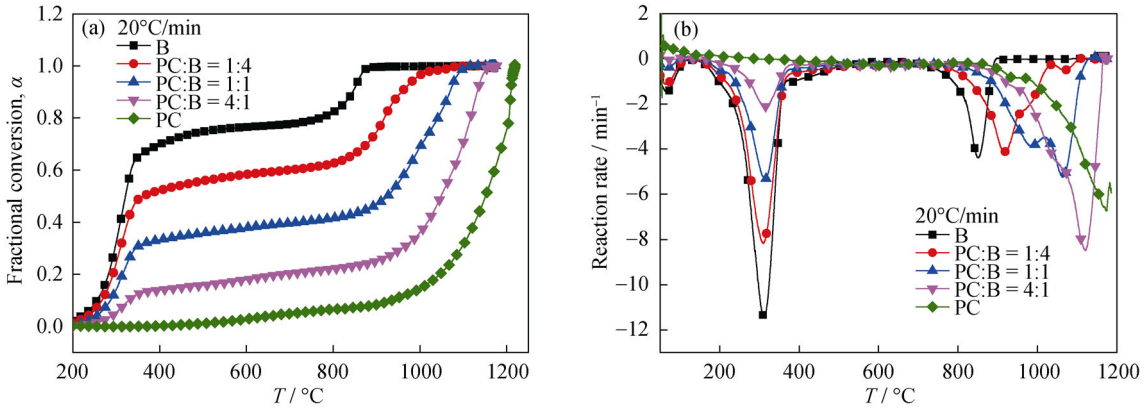

Fig. 3. Effect of blend ratio on the thermal behavior of samples at β = 20°C/min: (a) fractional conversion curves; (b) reaction rate curves.

Table 3. Characteristic gasification parameters of samples at different heating rates

Heating rate / (°C·min^{-1})	Sample	Pyrolysis stage		Char gasification stage		
		T_{max} / °C	DTG$_{max}$ / (min^{-1})	T_{max} / °C	DTG$_{max}$ / (min^{-1})	Temperature range / °C
5	PC	—	—	1078.4	2.05	852–1150
	PC:biomass = 4:1	300.6	0.63	1071.1	2.54	830–1097
	PC:biomass = 1:1	301.3	1.72	914.4	1.83	769–1020
	PC:biomass = 1:4	303.0	2.74	866.8	1.54	735–984
	biomass	303.6	3.24	800.5	1.78	679–841
10	PC	—	—	1150.5	3.81	830–1218
	PC:biomass = 4:1	308.2	1.22	1132.5	4.74	811–1160
	PC:biomass = 1:1	305.1	2.79	1026.1	2.97	789–1079
	PC:biomass = 1:4	310.0	4.35	894.1	2.54	764–983
	biomass	307.7	5.94	827.6	3.06	731–854
20	PC	—	—	1174.5	6.74	889–1253
	PC:biomass = 4:1	315.7	2.12	1121.7	8.48	845–1172
	PC:biomass = 1:1	314.8	5.34	1065.5	5.24	808–1139
	PC:biomass = 1:4	306.2	8.16	918.9	4.11	751–1033
	biomass	312.8	11.38	851.3	4.38	716–901

According to the results in Table 3, the gasification of PC and biomass occurred in different temperature ranges. The gasification of PC started when the gasification of biomass ended. Thus, the gasification of PC and biomass occurred successively, not simultaneously [11]. In the pyrolysis stage, DTG$_{max}$ increased with increasing biomass ratio. In the char gasification stage, the DTG$_{max}$ reached a maximum at all heating rates in the case of the sample mixed in a PC:biomass ratio of 4:1. The value of DTG$_{max}$ then decreased as the ratio of biomass was increased further. The maximum reaction rate of PC was larger than that of biomass in the char gasification stage. As the heating rate was 5°C/min, the maximum reaction rate of PC was 2.05 min^{-1}, whereas it was 1.78 min^{-1} for biomass. The T_{max} decreased with increasing biomass ratio under all heating rates and blend ratios. The DTG$_{max}$ was proportional to the reactivity of the sample, whereas T_{max} was inversely proportional to the reactivity.

4.2. Effect of heating rate on gasification characteristics

The gasification reaction rate curves of different blend ratios at heating rates of 5, 10, and 20°C/min are presented in Fig. 4.

As shown in Fig. 4, the heating rate obviously influenced the gasification behavior. In the case of biomass, according to the fractional conversion curve, the conversion rate decreased with increasing heating rate under the same temperature. The heating rate affected the shape and position of

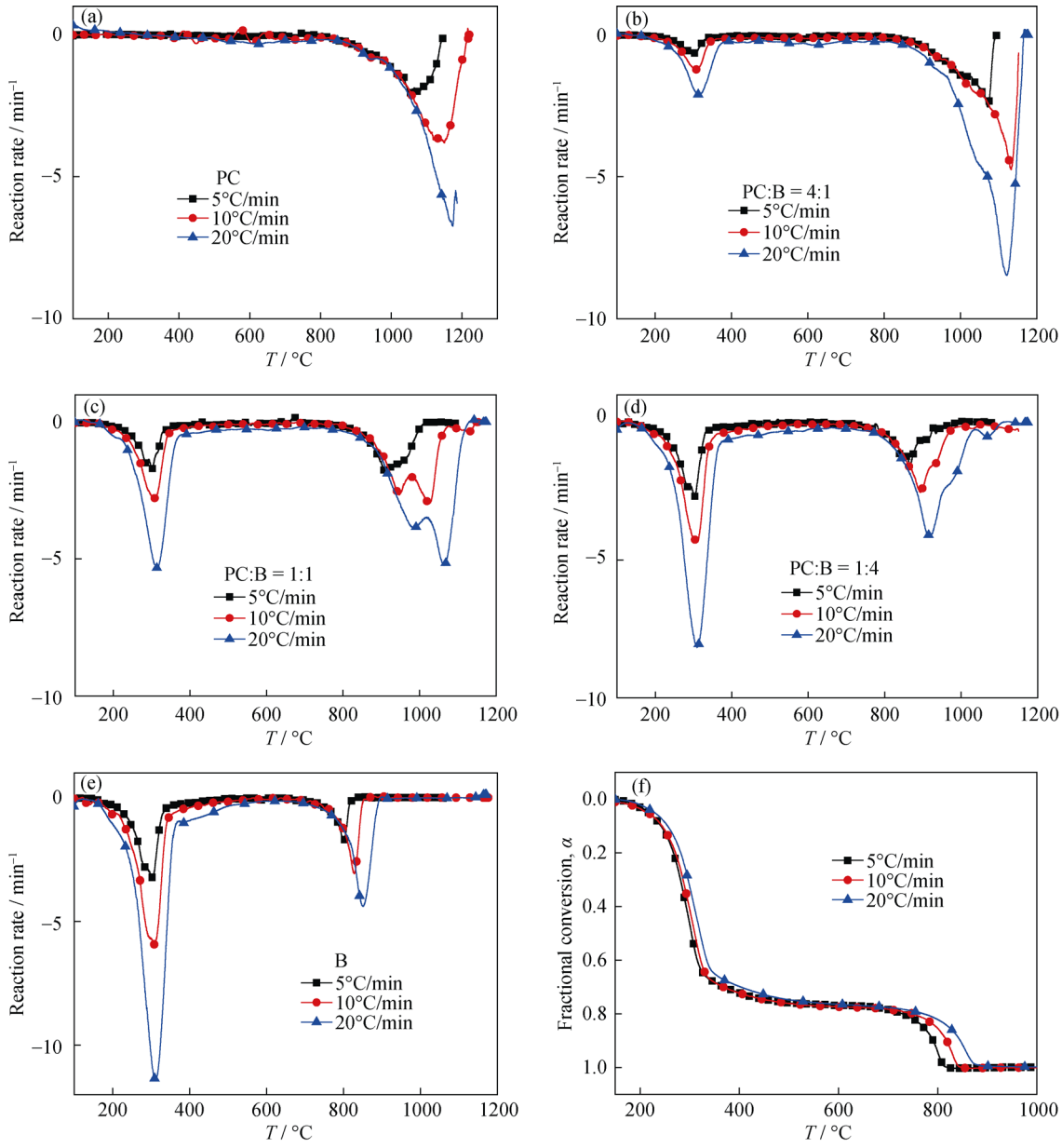

Fig. 4. Reaction rate curves of samples at different heating rates: (a) PC; (b) PC:biomass = 4:1; (c) PC:biomass = 1:1; (d) PC:biomass = 1:4; (e) biomass; (f) fractional conversion curve of biomass.

the reaction rate curves. With increasing heating rate, the reaction rate curves shifted to higher temperatures. On the one hand, the gasification reaction requires sufficient time to proceed to completion. However, with an increase of the heating rate, the time available at a given temperature was shortened. Therefore, the char gasification stage did occurred at higher temperatures. On the other hand, a heat hysteresis effect led to a temperature difference between the inside and outside of the particles; this thermal hysteresis phenomenon would be aggravated by an increase in the heating rate, which would also lead to a shift of the char gasification stage to higher temperatures [20]. With increasing heating rate, the gasification characteristic parameters (DTG_{max} and T_{max}) also increased. In addition, the temperature at which the reaction started decreased, whereas the temperature at which the reaction ended increased. In the case of biomass, as the heating rate was increased from 5°C/min to 20°C/min, indexes T_{max} and DTG_{max} increased from 800.5°C and 1.78 min^{-1} to 851.3°C and 4.38 min^{-1}, respectively. We concluded that gasification characteristics were improved by an increase of the heating rate.

4.3. Synergistic effect between PC and biomass

The synergistic effect between PC and biomass was

studied by comparing experimental and calculated reaction rate data. The calculated data were calculated according to the additive effect. The experimental and calculated reaction rate data collected at a heating rate of 5°C/min are shown in Fig. 5. The calculated reaction rate curves are basically consistent with the experimental curves in the pyrolysis stage, whereas a certain deviation between the calculated and experimental values is evident in the char gasification stage. Compared with the calculated reaction rate curves, the experimental reaction rate curves shifted to lower temperatures and also exhibited a larger peak value. According to the results in Table 3, with increasing biomass ratio, the DTG_{max} increased and T_{max} decreased. These results demonstrate that a synergistic effect exists between the PC and biomass. The reactivity of PC increased with the addition of biomass.

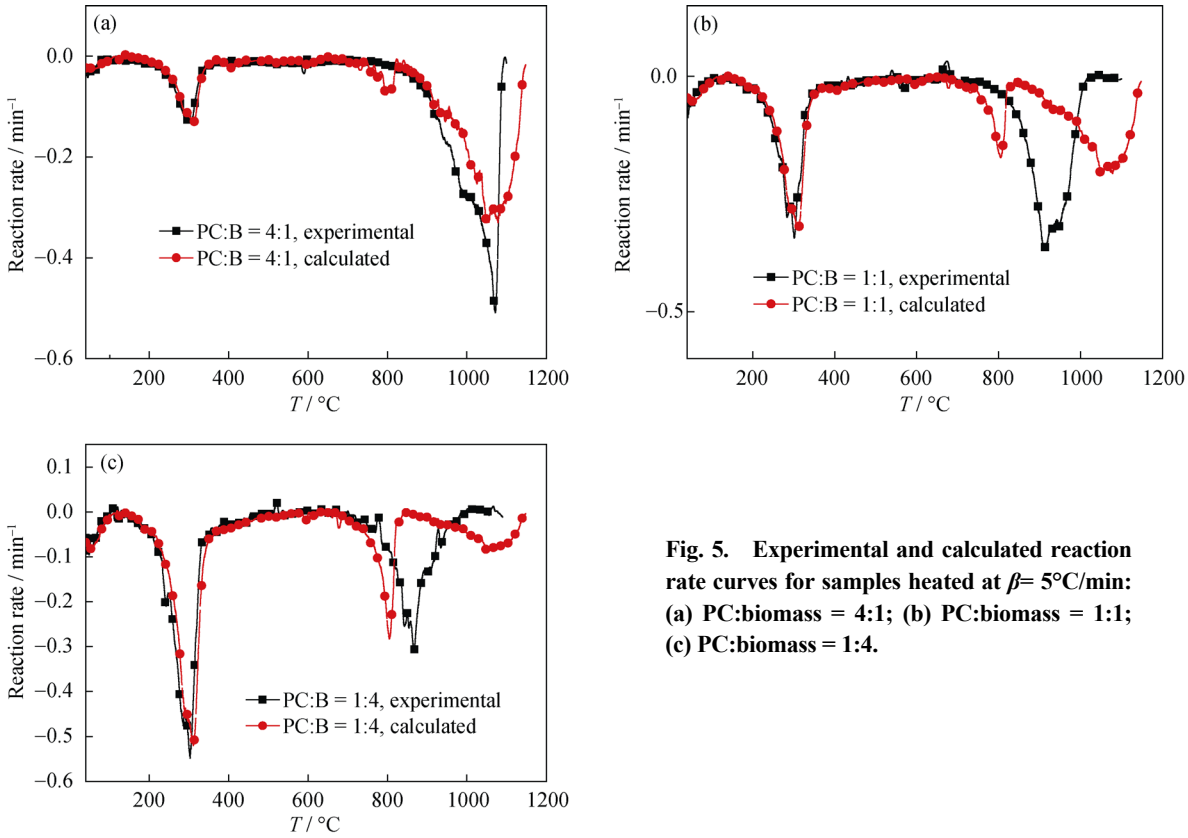

Fig. 5. Experimental and calculated reaction rate curves for samples heated at β= 5°C/min: (a) PC:biomass = 4:1; (b) PC:biomass = 1:1; (c) PC:biomass = 1:4.

Edreis *et al.* [9] and Wang *et al.* [21] proposed a root mean square (RMS) synergy index based on experimental and calculated reaction rate data to quantify the synergistic effect in the char gasification stage. The RMS values increased when the synergetic effect was more obvious. The RMS values under different blend ratios are shown in Fig. 6. With increasing biomass ratio, the deviation between the calculated and experimental values of reaction rate increased; the RMS values also increased at all heating rates.

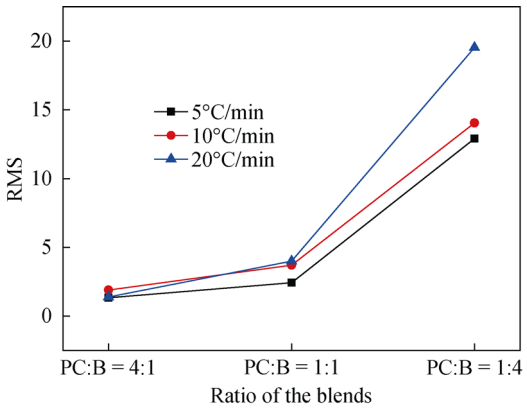

Fig. 6. RMS values for different blend ratios.

The synergistic effect observed between PC and biomass could contribute to the ash in the biomass [22]. The ash analysis results for PC and biomass are summarized in Table 2. The content of alkali and alkaline-earth metals in the biomass ash was as high as 56.5%. These elements have been demonstrated to act as catalysts in the gasification reaction [23]. The contents of CaO and SO_3 in the PC were high.

With increasing biomass ratio, the ash content in the blends increased, leading to a more obvious catalytic effect. The conversion rate then increased rapidly, and the time required for completion of the gasification reaction was shortened.

The synergistic effect may also be caused by the high volatiles content and the high reactivity of the biomass. When the PC and biomass co-gasification is conducted in the thermobalance, the biomass pyrolyzes rapidly. The volatiles may not only react with biomass but also with PC, thereby promoting the gasification of PC [9].

4.4. Kinetics analysis

In this paper, the KAS method was used to calculate the activation energy. One hundred different conversion rates ranging from 0.11 to 0.99 were chosen for the calculation of the activation energy. The activation energy was calculated according to Eq. (6). A plot of $\ln(\beta/T^2)$ vs. $1/T$ under several different conversion rates is shown in Fig. 7.

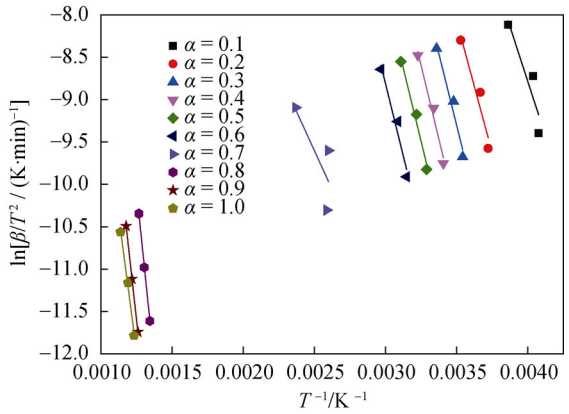

Fig. 7. Plot for determining the activation energy of gasification at different α values by the KAS method.

The activation energy of the samples are shown in Fig. 8. The activation energy in the pyrolysis stage was less than that in the char gasification stage under different blend ratios, demonstrating that the pyrolysis of char occurred much more easily than its gasification. In the pyrolysis stage, the activation energy of all the blend ratios exhibited the same trend in that they first increased and then decreased. However, the conversion rate that corresponds to the maximum activation energy differed for each blend ratio. In the cases of PC:biomass = 4:1, 1:1 and 1:4, the conversion rates at which the maximum activation energy occurred were 0.1, 0.2, and 0.3, respectively. For biomass, the activation energy reached a maximum when the conversion rate was 0.4 because of the breakage of macromolecular bonds at the low conversion rate, thus resulting in an increase in the activation energy [24]. With increasing conversion rate, the activation energy decreased, indicating that temperature was the main factor limiting pyrolysis [25]. These results suggest that the pyrolysis behavior changed with the conversion rate, which was similar to the results reported by Wang and Zhao [25].

In the char gasification stage, with the exception of the blend ratio of PC:biomass = 1:4, the activation energy of other blend ratios first decreased and then increased. For different blend ratios, the conversion rate at the beginning of the gasification reaction differed. When PC began to gasify, the conversion rate was 0.1. When the blend ratio PC:biomass = 4:1, 1:1 and 1:4, the conversion rate was 0.3, 0.5, and 0.6, respectively. For biomass, the conversion rate was 0.8. Thus, with increasing ratio of biomass, the conversion rate at the beginning of gasification increased gradually. This trend is attributed to the volatile content also increasing with increasing biomass ratio; the greater volatile content resulted in greater weight loss in the pyrolysis stage.

The activation energy of samples during the pyrolysis and char gasification stages is summarized in Table 4. In the pyrolysis stage, for the blend ratio of PC:biomass = 4:1, the activation energy was 64.4–76.7 kJ/mol, whereas it was 11.2–62.8 kJ/mol for biomass. In the char gasification stage, the activation energy was 129.1–177.8 kJ/mol for PC, whereas it was 120.3–150.5 kJ/mol for biomass.

To compare two different isoconversional methods (KAS and FWO methods), we calculated the activation energy of biomass by selecting 10 different fractional conversion values: 0.1, 0.2, 0.3, 0.4, 0.5, 0.6, 0.7, 0.8, 0.9, and 1.0. The activation energy calculated by different methods are illustrated in Fig. 9.

As evident in Fig. 9, the changes in the activation energy of biomass calculated using the KAS and FWO methods exhibited the same trend. However, the activation energy calculated by the FWO method were larger than those calculated by the KAS method. When the conversion was 1.0, the activation energy was 106.2 kJ/mol when calculated by the KAS method, whereas it was 120.3 kJ/mol when calculated by the FWO method. The difference between them is less than 14 kJ/mol. This result is similar to the results reported by Xiao *et al.* [18]. The difference was caused by the different mathematical methods used to solve the dynamics integral equations; i.e., the approximate processing method for integrating was different for the two isoconversional methods, which resulted in a slightly larger activation energy calculated using the FWO method [26].

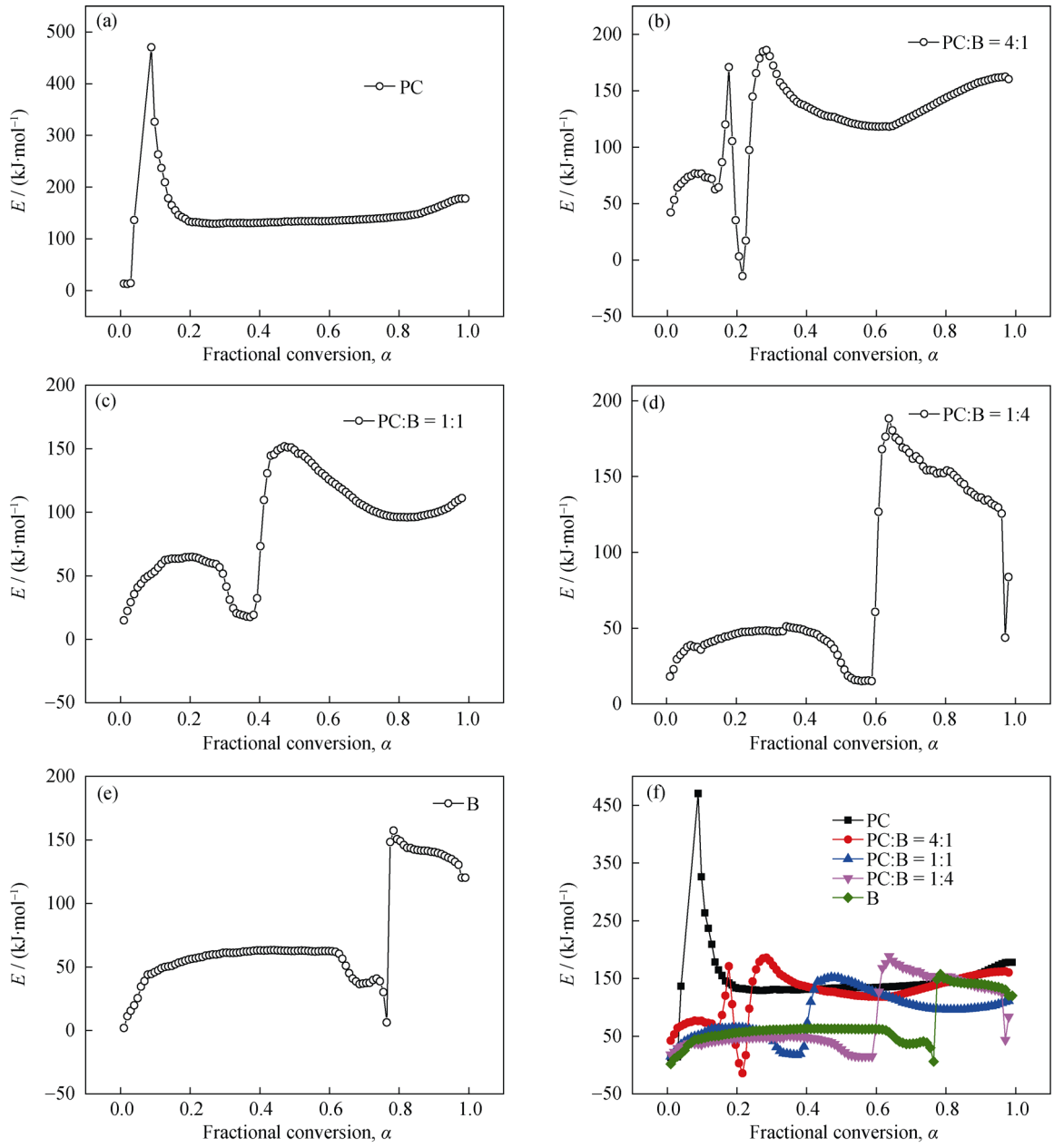

Fig. 8. Dependence of the activation energy (E_a) on α during the co-gasification stage, as determined using the KAS method: (a) PC; (b) PC:biomass = 4:1; (c) PC:biomass = 1:1; (d) PC:biomass = 1:4; (e) biomass; (f) all blends.

Table 4. Activation energy of samples in the pyrolysis and char gasification stages kJ/mol

Stage	PC	PC:biomass = 4:1	PC:biomass = 1:1	PC:biomass = 1:4	biomass
Pyrolysis stage	—	64.4–76.7	15.6–51.2	15.0–64.7	11.2–62.8
Char gasification stage	129.1–177.8	118.2–180.6	125.6–180.4	96.1–151.9	120.3–150.5

5. Conclusions

(1) The co-gasification of PC and biomass was studied in this work. The results indicated that gasification of PC occurs in a single stage, whereas gasification of biomass and the blends occurs in two stages: pyrolysis and char gasification. With increasing heating rate, the reaction rate curve gradually shifts to higher temperatures and the characteristic gasification parameters are also increased. A synergistic effect occurs during PC and biomass co-gasification; this effect is attributed to the alkali and alkaline-earth metals in biomass ash and also to the high volatile content in biomass.

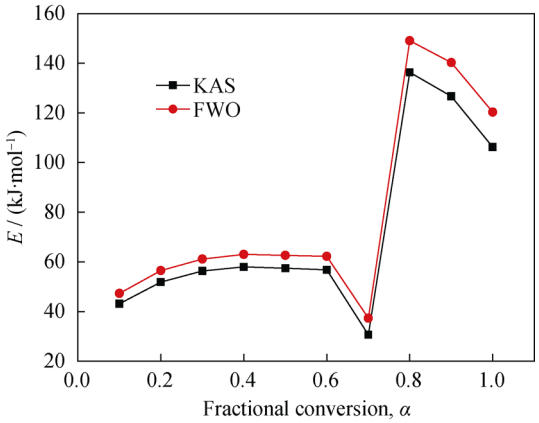

Fig. 9. Activation energy (E_a) calculated by the KAS and FWO methods at different α values.

(2) According to the kinetics analysis, the activation energy of the pyrolysis stage is less than that of the char gasification stage. In the char gasification stage, the activation energy is 129.1–177.8 kJ/mol for PC, whereas it is 120.3–150.5 kJ/mol for biomass. Two isoconversional methods (FWO and KAS methods) were used to calculate the activation energy of biomass in the char gasification stage. The results showed that the activation energy calculated by both methods exhibited the same trend. However, the activation energy calculated by the FWO method were larger than those calculated by the KAS method. When the conversion was 1.0, the activation energy was 106.2 kJ/mol, as calculated by the KAS method, whereas it was 120.3 kJ/mol calculated by the FWO method; the difference between these values is less than 14 kJ/mol.

Acknowledgements

This work was supported by the Fundamental Research Fund for the Central Universities of China (FRF-TP-15-063A1) and the 111 Project (No. B13004).

References

[1] L. Kolbeinsen, Modelling of DRI processes with two simultaneously active reducing gases, *Steel Res. Int.*, 81(2010), No. 10, p. 819.

[2] M.F. Irfan, A. Arami-Niya, M.H. Chakrabarti, W.M. Ashri Wan Daud, and M.R. Usman, Kinetics of gasification of coal, biomass and their blends in air (N_2/O_2) and different oxy-fuel (O_2/CO_2) atmospheres, *Energy*, 37(2012), No. 1, p. 665.

[3] X.L. Zhan, J. Jia, Z.J. Zhou, and F.C. Wang, Influence of blending methods on the co-gasification reactivity of petroleum coke and lignite, *Energy Convers. Manage.*, 52(2011), No. 4, p. 1810.

[4] X.L. Zhan, Z.J. Zhou, and F.C. Wang, Catalytic effect of black liquor on the gasification reactivity of petroleum coke, *Appl. Energy*, 87(2010), No. 5, p. 1710.

[5] R. Zanzi, K. Sjöström, and E. Björnbom, Rapid high-temperature pyrolysis of biomass in a free-fall reactor, *Fuel*, 75(1996), No. 5, p. 545.

[6] H.B. Zuo, W.W. Geng, J.L. Zhang, and G.W. Wang, Comparison of kinetic models for isothermal CO_2 gasification of coal char-biomass char blended char, *Int. J. Miner. Metall. Mater.*, 22(2015), No. 4, p. 363.

[7] J.L. Zhang, J. Li, Z.W. Hu, Y.Q. Fu, and H.B. Zuo, Catalytic gasification reaction and kinetics of deashing biomass char, *J. Univ. Sci. Technol. Beijing*, 35(2013), No. 11, p. 1431.

[8] G.W. Wang, J.L. Zhang, X.M. Hou, J.G. Shao, and W.W. Geng, Study on CO_2 gasification properties and kinetics of biomass chars and anthracite char, *Bioresour. Technol.*, 177(2015), p. 66.

[9] E.M.A. Edreis, G.Q. Luo, A.J. Li, C.F. Xu, and H. Yao, Synergistic effects and kinetics thermal behaviour of petroleum coke biomass blends during H_2O co-gasification, *Energy Convers. Manage.*, 79(2014), p. 355.

[10] E.M.A. Edreis, G.Q. Luo, A.J. Li, C. Chao, H.Y. Hu, S. Zhang, B. Gui, L. Xiao, K. Xu, P.G. Zhang, and H. Yao, CO_2 co-gasification of lower sulphur petroleum coke and sugar cane bagasse via TG-FTIR analysis technique, *Bioresour. Technol.*, 136(2013), p. 595.

[11] V. Nemanova, A. Abedini, T. Liliedahl, and K. Engvall, Co-gasification of petroleum coke and biomass, *Fuel*, 117(2014), p. 870.

[12] J. Fermoso, B. Arias, M.V. Gil, M.G. Plaza, C. Pevida, J.J. Pis, and F. Rubiera, Co-gasification of different rank coals with biomass and petroleum coke in a high-pressure reactor for H_2-rich gas production, *Bioresour. Technol.*, 101(2010), No. 9, p. 3230.

[13] J. Fermoso, B. Arias, B. Moghtaderi, C. Pevida, M.G. Plaza, J.J. Pis, and F. Rubiera, Effect of co-gasification of biomass and petroleum coke with coal on the production of gases, *Greenh. Gases. Sci. Technol.*, 2(2012), No. 4, p. 304.

[14] J. Fermoso, B. Arias, M.G. Plaza, C. Pevida, F. Rubiera, J.J. Pis, F. García-Peña, and P. Caser, High-pressure co-gasification of coal with biomass and petroleum coke, *Fuel Process. Technol.*, 90(2009), No. 7-8, p. 926.

[15] G.Y. Xu and G.G. Sun, Study on characteristics of co-gasification of biomass and petroleum coke, *J. Fuel Chem. Technol.*, 39(2011), No. 6, p. 438.

[16] J.L. Zhang, G.W. Wang, J.G. Shao, and H.B. Zuo, A modified random pore model for the kinetics of char gasification, *Bioresources*, 9(2014), No. 2, p. 3497.

[17] M.J. Starink, The determination of activation energy from linear heating rate experiments: a comparison of the accuracy of isoconversion methods, *Thermochim. Acta*, 404(2003), No. 1-2, p. 163.

[18] H.M. Xiao, X.Q. Ma, and Z.Y. Lai, Isoconversional kinetic analysis of co-combustion of sewage sludge with straw and coal, *Appl. Energy*, 86(2009), No. 9, p. 1741.

[19] J.H. Flynn and L.A. Wall, A quick direct method for deter-

mination of activation energy from thermogravimetric data, *J. Polym. Sci., Part B*, 4(1966), No. 5, p. 323.

[20] G.W. Wang, J.L. Zhang, J.G. Shao, and S. Ren, Characterisation and model fitting kinetic analysis of coal/biomass co-combustion, *Thermochim. Acta*, 591(2014), p. 68.

[21] Q. Wang, W.Z. Zhao, H.P. Liu, C.X. Jia, and S.H. Li, Interactions and kinetic analysis of oil shale semi-coke with cornstalk during co-combustion, *Appl. Energy*, 88(2011), No. 6, p. 2080.

[22] R. Habibi, J. Kopyscinski, M.S. Masnadi, J. Lam, J.R. Grace, C.A. Mims, and M.H. Josephine, Co-gasification of biomass and non-biomass feedstocks: synergistic and inhibition effects of switchgrass mixed with sub-bituminous coal and fluid coke during CO_2 gasification, *Energy Fuels*, 27(2013), No. 1, p. 494.

[23] G. Pu, W.L. Zhu, H.P. Zhou, Y.G. Liu, and Z.R. Zhang, Kinetics of co-gasification of low-quality lean coal and biomass, *Bioresources*, 10(2015), No. 2, p. 2773.

[24] S.S. Kim, J. Kim, J.K. Jeon, Y.K. Park, and C.J. Park, Non-isothermal pyrolysis of the mixtures of waste automobile lubricating oil and polystyrene in a stirred batch reactor, *Renewable Energy*, 54(2013), p. 241.

[25] J.X. Wang and H.B. Zhao, Thermogravimetric analysis of rubber glove pyrolysis by different iso-conversional methods, *Waste Biomass Valorization*, 6(2015), No. 4, p. 527.

[26] Y. Zheng, B.H. Chi, B.W. Wang, and C.G. Chu, Application and comparison of equal conversion rate methods in the decomposition kinetics research, *Coal Convers.*, 29(2006), No. 4, p. 34.